

Air Separation Membranes: An Alternative to EGR in Large Bore Natural Gas Engines

Munidhar Biruduganti

Sreenath Gupta

Bipin Bihari

Steve McConnell

Raj Sekar

Argonne National Laboratory,
Argonne, IL 60439

Air separation membranes (ASMs) could potentially replace exhaust gas recirculation (EGR) technology in engines due to the proven benefits in NO_x reduction but without the drawbacks of EGR. Previous investigations of nitrogen-enriched air (NEA) combustion using nitrogen bottles showed up to 70% NO_x reduction with modest 2% nitrogen enrichment. The investigation in this paper was performed with an ASM capable of delivering at least 3.5% NEA to a single-cylinder spark-ignited natural gas engine. Low temperature combustion is one of the pathways to meet the mandatory ultra low NO_x emissions levels set by regulatory agencies. In this study, a comparative assessment is made between natural gas combustion in standard air and 2% NEA. Enrichment beyond this level degraded engine performance in terms of power density, brake thermal efficiency (BTE), and unburned hydrocarbon emissions for a given equivalence ratio. The ignition timing was optimized to yield maximum brake torque for standard air and NEA. Subsequently, conventional spark ignition was replaced by laser ignition (LI) to extend lean ignition limit. Both ignition systems were studied under a wide operating range from ψ : 1.0 to the lean misfire limit. It was observed that with 2% NEA, for a similar fuel quantity, the equivalence ratio (Ψ) increases by 0.1 relative to standard air conditions. Analysis showed that lean burn operation along with NEA and alternative ignition source, such as LI, could pave the pathway for realizing lower NO_x emissions with a slight penalty in BTE. [DOI: 10.1115/1.4000296]

1 Introduction

The availability of clean sustainable energy to fuel the ever-increasing use of energy-hungry prime movers is one of the most critical challenges encountered by mankind. Alongside fuel reserves concerns, atmospheric pollution caused by anthropogenic activities, especially as a result of energy consumption, has become a topic of extensive discussion and deliberation. Nitrogen oxides emissions, or collectively known as NO_x , are a major contributor to photo-chemical smog present in urban areas. It has severe health repercussions, which if left unchecked, could potentially risk millions of lives. The U.S. Environmental Protection Agency (EPA) estimates that 59% of NO_x emissions come from on-road and off-road vehicles, 22% from power generation (electric utilities), and the remaining 19% from industrial, commercial, and residential sources [1]. Due to its serious health and environmental impact, the reduction in NO_x in our atmosphere has become a major focus in the fight against air pollution. Some of the emissions reducing combustion concepts currently being studied include HCCI, alternative ignition systems, such as pilot fuel ignition, laser ignition (LI), etc., besides low temperature combustion (LTC) strategies, each with inherent advantages and limitations [2–6].

2 Benefits of Air Separation Membranes Compared to EGR

Stationary natural gas fired reciprocating engines are used for electrical power generation and oil-field pumping applications, most of which are spark-ignited. These large bore engines are required to have high reliability levels due to round-the-clock operation. Exhaust gas recirculation (EGR) has proved to be a very

effective tool to reduce in-cylinder temperature and hence NO_x , since NO_x is a strong function of temperature. However, EGR has several built-in adverse ramifications that negate its advantages in the long term. Some of them include:

- combustion contamination
- greater control system complexity
- application variability
- material durability
- decreased fuel economy
- lubricant contamination
- increased PM emissions

Nitrogen enriched air (NEA) is an effective alternative to EGR without its undesired consequences. This could be achieved by using a mature technology, which involves selective permeation of gases with an air separation membrane (ASM) shown in Fig. 1 [7]. Oxygen-rich and nitrogen-rich streams are produced by pumping air through a nonporous polymeric membrane. The basic principle of membrane operation and various designs and operating characteristics are described in Ref. [8]. Research work done on a locomotive two stroke diesel engine by Poola and Sekar [9] corroborate a variable air technique to reduce emissions. Introduction of inert diluents, such as nitrogen, into a fuel-air mixture slow down the reaction rates of participating chemical species, which eventually lower combustion temperatures and hence lower NO_x . This process gives an added control parameter to reduce combustion temperature in advanced engines.

3 Laser Ignition

The demand for high thermal efficiency, specific power, and lower emissions favors operation of natural gas engines under turbocharged lean burn conditions [10]. Under such conditions, the gas charge attains high enough density at the time of ignition, which has an insulating effect between the electrodes of a spark plug. These conditions entail the use of very high voltages

Contributed by the IC Engine Division of ASME for publication in the JOURNAL OF ENGINEERING FOR GAS TURBINES AND POWER. Manuscript received May 21, 2009; final manuscript received June 11, 2009; published online May 27, 2010. Editor: Dilip R. Ballal.

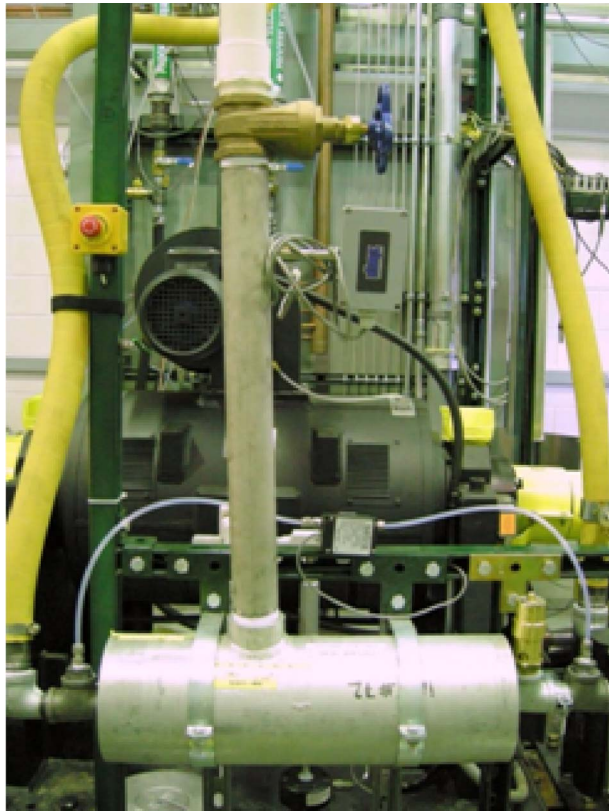


Fig. 1 Air separation membrane

(≥ 40 kV) to increase the probability of ignition. Current spark ignition (SI) systems experience reliability issues at such high voltages across the spark plug electrodes. Additionally, the spark plug electrodes erode over time requiring spark gap adjustment every 1000–4000 hrs of operation [9]. With a goal to reduce engine downtime, there has been a push in natural gas engine industry to increase maintenance intervals to 8000 hrs.

In spite of the many improvements that have taken place over the past two decades in ignition hardware [11], conventional coil based ignition systems are unable to meet the above demands. As a result, there has been a thrust to investigate alternate ignition strategies. Some of the ignition systems studied for natural gas engines are HCCI [12,13], pilot assisted (dual fuel) ignition [4–6,13], plasma rail [14], and rail plug [15]. HCCI engines are limited by poor ignition and combustion control at higher loads while promising relatively low emissions at low loads [2]. Pilot ignited natural gas engines utilize a pilot fuel, usually diesel, to initiate combustion [3]. These engines take advantage of the high compression ratios of compression ignition (CI) engines and hence attain fairly higher brake thermal efficiency (BTE) [4]. The pilot quantity and injection timing plays an important role in engine performance and emissions [5]. However, these engines need a major hardware change for their functionality. Laser ignition, on the other hand, promises various performance benefits such as

- successful ignition at high pressures, which leads to reduced misfire, improved fuel efficiency, and lower unburned hydrocarbons (UHC) emissions
- lower maintenance as the requirement to maintain a reasonable spark gap is eliminated
- lower NO_x emissions due to fuel-lean operation
- shorter ignition delays or enhanced combustion rates, which allow retarded timing thereby reducing NO_x emissions
- reduced heat loss to the cylinder head due to ignition kernel location away from the walls, improving overall efficiency

Table 1 Engine details

Engine	Single cylinder, four stroke, SI
Bore (mm)	130
Stroke (mm)	140
Comp. ratio	11:1
Displacement (L)	1.857
Power (kW)	33
Speed (rpm)	1800
Ignition system	Capacitance discharge ignition (CDI) (Altronic, Inc.), Big Sky Laser

Previous attempts to use laser ignition in reciprocating engines has been recently reviewed in Ref. [16]. As mentioned in that paper, though significant benefits are imminent, LI systems are still in the developmental stage. In this study, LI was installed on a natural gas engine to quantify the benefits it offers compared with spark ignition.

4 Experimental Setup

A single-cylinder EngineTech (RSi130Q) spark-ignited natural gas research engine was used to investigate nitrogen-enriched combustion via an air separation membrane. A very detailed description of the experimental setup was published in an earlier paper [17]. The engine details are included in Table 1, and Fig. 2 shows the schematic arrangement of the experiment.

The major change in experimental setup compared with previous work [17] was the installation of CompAire natural gas compressor, which compressed the Argonne site wide natural gas supply pressure from 5 psi (gauge) to 130 psi (gauge). Previously, an array of natural gas bottles was used to fuel the engine whose composition was slightly different from the current supply source. Therefore, the stoichiometric air/fuel ratio changed from 16.2 to 16.39. Also, gas injection pressure dropped by about 15 psi (gauge). Natural gas flow rate was measured with a Micro Motion Coriolis-type flow meter. Natural gas was introduced into the engine intake manifold using an injector block consisting of two electronically-controlled gas injectors (CAP, Inc., Poway, CA). Gas delivery was adjusted by a pulse-width modulation-controlled solenoid. In order to reduce UHC, the injection event was triggered by a timing disk to prevent natural gas from being “short-circuited” to the exhaust during the valve overlap period. Due to the drop in injection pressure, the pulse-width duration was adjusted to attain previously observed fuel flow rates.

High-speed in-cylinder pressure was measured using a Kistler 6013B pressure transducer mounted on the cylinder head. The pressure signal was phased with respect to crank angle using an optical shaft encoder (Kistler) coupled to the engine crankshaft. The transducer was connected to a data acquisition system (Win600e) to do combustion analysis via charge amplifier (Kistler) which converted the charge signal into a voltage signal.

Horiba MEXA-7100D, an integrated five-gas analyzer emissions bench, was used for CO , CO_2 , NO_x , UHC, and O_2 measurement. A heated flame ionization detector and a heated chemiluminescent detector were used for HC and NO_x emissions measurements, respectively. O_2 concentration was measured with a paramagnetic analyzer, while CO and CO_2 were measured using infrared analyzers.

Variation of the O_2 enriched air, as shown in Fig. 2, (permeate) created partial pressures in ASM, which facilitated separation and produced the desired NEA (retentate). This NEA was supplied to the engine. O_2 concentration within the NEA supplied to the engine was measured by an O_2 analyzer to adjust nitrogen enrichment levels systematically.

An Altronic CD200 ignition module helped vary ignition timing between 10 deg and 40 deg before top dead center (BTDC). Baseline SI tests were followed by LI for the given test matrix presented in Table 2. An ultracompact folded resonator (CFR) Nd:

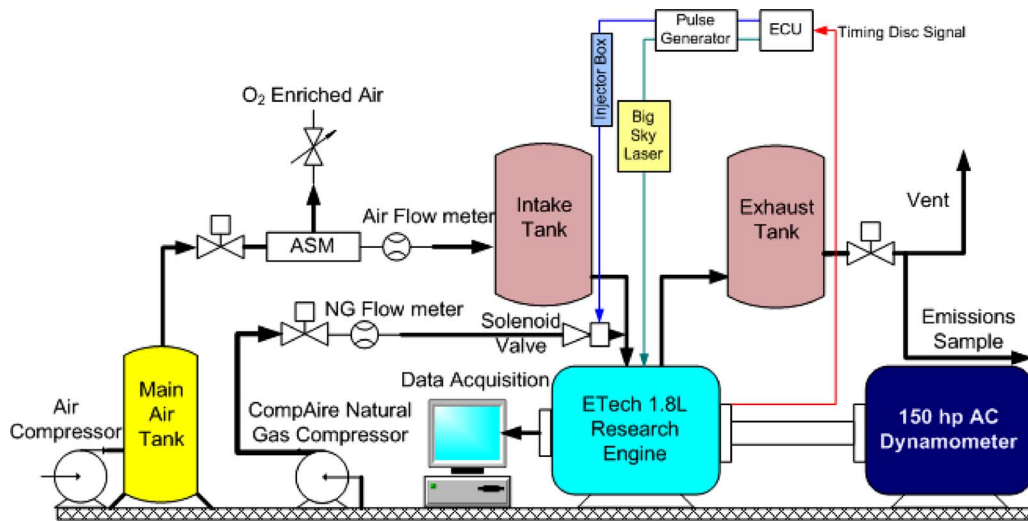


Fig. 2 Schematic of experimental setup

YAG laser (Big Sky Laser, Montana) capable of delivering a 532 nm laser pulse with energy of 31 mJ/pulse was used as the laser source for the experiment. The Altronic system was used to trigger the laser ignition system. High-power laser pulses were transmitted directly to a “laser plug” installed on the cylinder head. The laser plug focuses the transmitted laser pulses to generate fluences of $\sim 10^{12}$ W/cm² in order to achieve gas breakdown [18]. The focal distance was 13 mm away from the laser plug tip. Figure 3 shows a photograph of the spark plug and the laser plug. The spark plug used is a standard 18 mm spark plug with 0.51 mm spark gap.

5 Results and Discussion

The objectives of this effort were as follows:

- to quantify the NO_x reduction benefit by supplying NEA with an ASM
- to compare engine performance between standard air and NEA supplied through an ASM
- to extend lean combustion limit by alternative ignition source, such as lasers, both with and without NEA
- to demonstrate the advantages of lean burn engine operation

The test matrix (shown in Table 2) was developed based on typical stationary engine operating conditions for most generator and CHP applications, i.e., constant speed of 1800 rpm and engine full load measured as brake mean effective pressure (BMEP): 12 bar (33 kW at 1800 rpm).

Complete control of ignition timing, fuel flow, air flow, and nitrogen enrichment allowed judicious choice of operating conditions. Intake and exhaust back pressure control facilitated simulated turbocharged conditions assuming 60% turbocharger efficiency. Intake air pressure and exhaust back pressure was adjusted using two pneumatically-controlled valves with PID controllers. Although boost air temperature control was not incorporated, it was believed that an intercooler (downstream of the compressor in a production engine) could mimic inlet charge conditions observed in this study.

ASM installation alters the composition of standard air based on the level of partial pressures maintained across the membrane fibers. O₂, being relatively more permeable than N₂, permeates through the membrane fibers (coated with a polymeric material) to yield a permeate flow (O₂ enriched air (OEA)) and retentate flow (nitrogen-enriched air). This parameter is varied by opening or closing the permeate flow valve shown in Fig. 2. In order to make an accurate comparison between the two technologies studied, i.e., standard air and NEA, the conventional definition of Φ was redefined to reflect only the O₂ to fuel ratio. Equivalence ratio (Φ), traditionally, is defined as the ratio of actual (measured) fuel flow to air flow ratio to the stoichiometric fuel flow to air flow ratio. However, since the experiments in this work modified the chemical composition of air, an O₂ based equivalence ratio (ψ) is introduced. It is believed to bring clarity for performance comparison due to the variation in O₂/N₂ ratio in air. It is represented by the following formula:

$$\psi = \frac{[\text{oxygen/fuel}]_{\text{stoic}}}{[\text{oxygen/fuel}]_{\text{actual}}} \quad (1)$$

According to this definition, the O₂/fuel ratio for stoichiometric conditions remains constant at 3.794 (based on natural gas C_{1.02943}



Fig. 3 Photograph of spark plug and laser plug

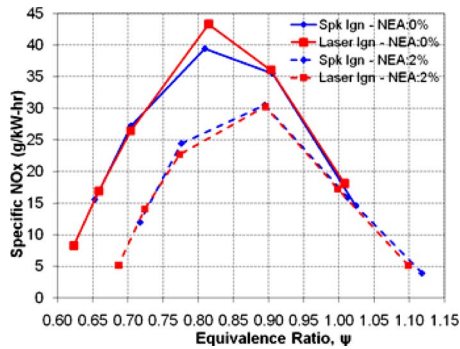


Fig. 4 Specific NO_x as a function of ψ

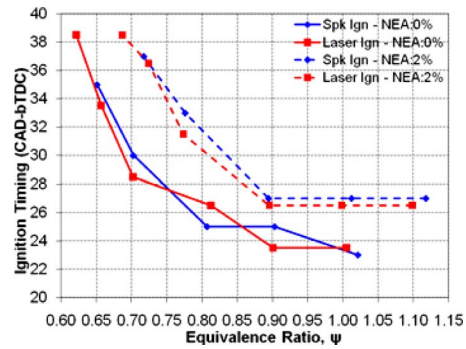


Fig. 5 Ignition timing as a function of ψ

H_{3,9925} supplied to Argonne). However, if the traditional equivalence ratio (Φ) was to be used, the air/fuel ratio for stoichiometric conditions would change from 16.3922 (standard air) to 18.072 (2% NEA) due to the amount of O₂ depletion in the intake air. O₂ flow rate was obtained by multiplying the O₂ mass fraction in the charge with the measured air flow rate. A correction factor of 0.9975 was used to compensate for the change in NEA density with respect to standard air for 2% NEA condition.

6 Engine Out Emissions

NEA is the air containing N₂ in excess of 79.05% (by volume). N₂ enrichment was attained by controlling the O₂ flow rate, as shown in the Fig. 2. Previous research showed that with NEA, NO_x reduction is proportional to engine load—NO_x reduction was greater for higher engine loads [19]. This is primarily due to the prevalent higher flame temperatures for higher engine loads. Hence, the present work was limited to evaluating the engine performance and behavior at the full load, 12 bar (BMEP). Also, acceptable engine operation was limited to below 3% NEA for near stoichiometric operation. In this study, only 2% NEA condition is discussed. Engine operating regime vis-à-vis equivalence ratio, Ψ , was varied from $\psi=1.0$ to lean misfire limit. The lean misfire limit was defined as the limit when coefficient of variation of indicated mean effective pressure (COV_{IMEP}) exceeded 5%. This is discussed at length in Secs. 7 and 8.

Figure 4 shows NO_x as a function of ψ at maximum brake torque (MBT) ignition timing for standard air and 2% NEA. Both conventional SI and LI are shown to depict the benefits and limitations of the respective systems. LI indeed offered the benefit of leaner operation and hence the lower NO_x compared with SI. For standard air, NO_x increased steadily going from $\psi:1.0$ to 0.81 and changed course on further leaning the charge. However, NO_x peaked at $\psi:0.9$ with 2% NEA for both SI and LI. Both these peak conditions for NO_x production occur at similar fueling rates. This can be explained by considering the fact that the NEA case becomes richer (higher equivalence ratio ψ) for a given fueling rate. For $\psi:0.81$, the drop in NO_x was 13 g/kWh for SI and 19 g/kWh for LI. The trends are fairly similar in both SI and LI. LI, however, extended ψ from 0.65 to 0.62 with standard air and from 0.72 to 0.68 with 2% NEA.

When 2% NEA is supplied with similar fueling rate as for stoichiometric standard air, ψ becomes fuel rich and loses power, BTE, and NO_x due to insufficient O₂ available for complete combustion of fuel. This reduces the bulk gas temperatures and therefore decreases NO_x. According to previous NO_x studies, NO_x is a strong function of combustion temperatures. Bulk gas temperature is an exponential component in the NO_x formation mechanism. Even a slight reduction of bulk gas temperature significantly alters NO_x formation. Another factor, which affects NO_x formation, is the O₂ content in a given mixture. Since nitrogen enrichment effectively depletes the net O₂ concentration, NO_x formation is sig-

nificantly reduced. With nitrogen enrichment the lean limits decrease considerably due to excessive unacceptable misfires, as shown in Fig. 4.

Attempts were made to maintain a constant BMEP while varying Ψ and nitrogen enrichment. This was done by varying the fuel flow and air flow proportionately to attain a specific Ψ for 12 bar BMEP. When 2% NEA was supplied to the engine for a given operating condition, the combustion reaction rates were decreased and delayed in the engine cycle. This led to loss in power and BTE. In order to attain MBT for a given operating condition, the heat release peak or 50% mass fraction burn (MFB) has to occur close to TDC. Therefore, the ignition timing was judiciously advanced, as shown in Fig. 5, to compensate for the delayed combustion phasing. SI and LI curves followed very similar trends. With NEA, ignition timing had to be advanced by 3 deg at $\Psi:1.0$ and close to 10 deg at $\Psi:0.7$.

Figure 6 shows BTE as a function of Ψ for both standard air and 2% NEA using SI and LI. It could be used effectively to compare the effect of NEA on BTE for both ignition systems. BTE is defined as the ratio of the brake power produced by the engine to the fuel energy feed rate based on the lower heating values of the fuel (natural gas). The power required for compressing intake air from ambient to engine intake pressures (103–250 kPa) was unaccounted in the BTE calculations and is beyond the scope of this study. It was assumed that a turbocharger could accommodate these conditions. It would be fairly reasonable to expect BTE corrections amounting to as high as 10% based on ASM installations on other engine platforms. It is therefore acknowledged that the actual BTE numbers would be lower in a practical standpoint. The pressure losses associated with using an ASM is shown in Fig. 7. The pressure drop across the ASM varied from 5.5 kPa to 7 kPa for passing standard air between $\Psi:0.65$ and 1.0 (O₂ valve closed in Fig. 2) and from 7 kPa to 9 kPa while passing 2% NEA between $\Psi:0.65$ and 1.0 (O₂ valve opened appropriately). It is also acknowledged that higher nitrogen enrichment would result in higher pumping losses.

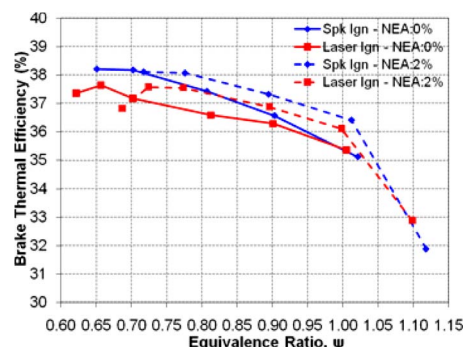


Fig. 6 BTE as a function of ψ

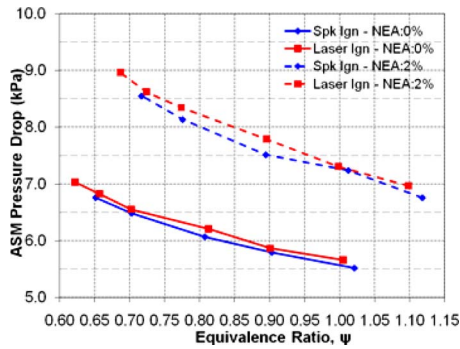


Fig. 7 ASM pressure drop as a function of ψ

Although the Fig. 6 shows that for a given Ψ , say, 0.81, BTE for 2% NEA is higher than for standard air, after accounting for parasitic losses (relative pressure drop of 2.5 kPa, Fig. 7) the trend lines would shift lower than the standard air conditions. These findings shall be presented in a later publication. As previously mentioned, nitrogen enrichment beyond stoichiometric condition resulted in excessive power and BTE penalty due to unavailability of O_2 for complete combustion of fuel. This is reflected very clearly in total unburned hydrocarbons, CO, and CO_2 emissions in Figs. 8–10, respectively. CO emissions increased beyond the analyzers measurement range for $\Psi > 1$, which could be higher than shown (60 g/kW h) due to incomplete oxidation of CO to CO_2 . UHC (Fig. 8) increased slightly between $\Psi: 0.8-1.0$ with 2%NEA for both SI and LI. However, UHC increased significantly as the mixture approached lean limits. The trends were similar for both ignition systems with LI extending the lean limit further to 0.62 (air) and 0.68 (2% NEA), respectively. This behavior also explains the drop in BTE at lean conditions for both ignition systems. BTE with LI was lower than SI, as seen in Fig. 6. It could be surmised that in the case of LI, the ignition kernel forms at a

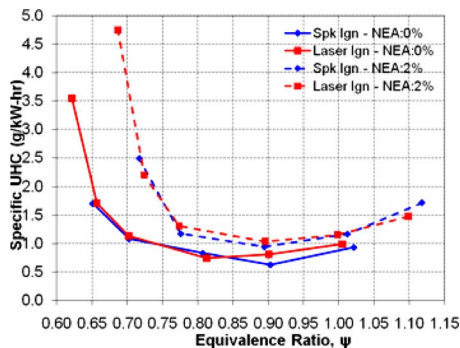


Fig. 8 Specific UHC as a function of ψ

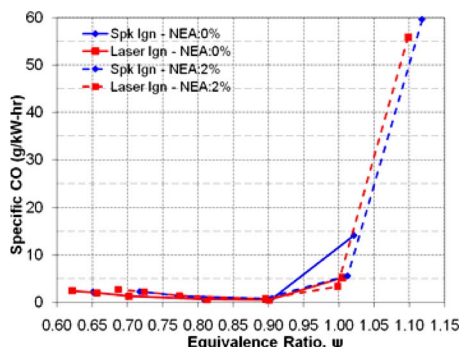


Fig. 9 Specific CO as a function of ψ

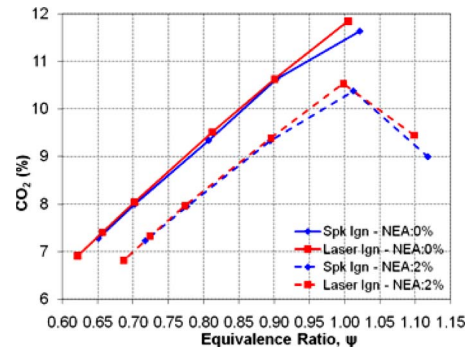


Fig. 10 Exhaust CO_2 as a function of ψ

nonoptimal location. Earlier LI studies at Argonne showed improvement in combustion and therefore better BTE. Further analysis shall be published addressing these challenges at a later time. However, in the present scope, there is a clear benefit associated with LI in terms of extension of lean limit. CO emissions (Fig. 9) also increased slightly with leaner mixtures accounting for unburned fuel in the exhaust and lower BTE.

It was observed (Fig. 10) that CO_2 emissions reduced significantly with NEA compared with standard air. Leaner operation becomes more attractive due to the current global warming concerns. CO_2 emissions reduced from 12% at stoichiometric conditions to less than 7% for the lean condition. Figure 11 shows the amount of O_2 available in the exhaust as a function of Ψ . This chart explains the need for an O_2 based equivalence ratio Ψ compared with the standard definition. It depicts that regardless of change in engine control variables such as ignition timing, % NEA, etc. for a given fuel to O_2 ratio, there can only be a proportionate amount of excess O_2 in the exhaust. Therefore, all data points for both standard air and 2% NEA follow a very consistent trend and confirm this approach.

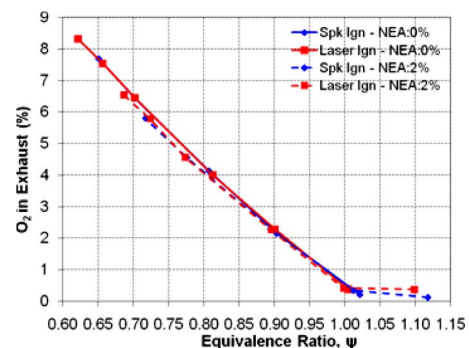


Fig. 11 Exhaust O_2 as a function of ψ

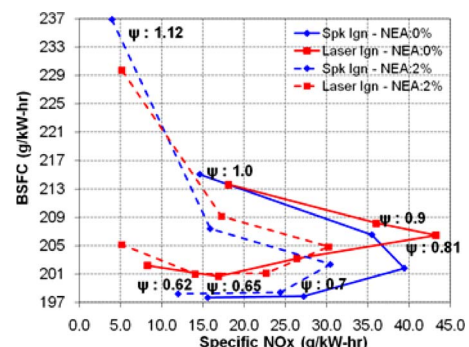


Fig. 12 BSFC versus specific NO_x at different ψ

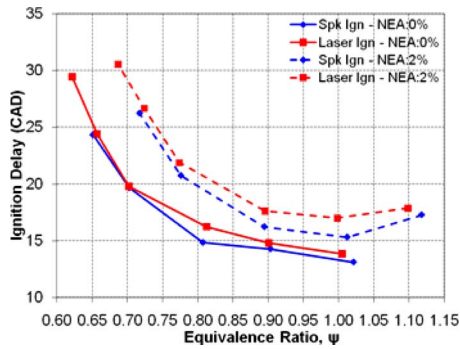


Fig. 13 Ignition delay as a function of ψ

Figure 12 shows a trade off chart between brake specific fuel consumption (BSFC) versus NO_x emissions for different Ψ comparing the effect of a combination of NEA and LI with its SI counterpart. Clearly, NEA reduces NO_x for all Ψ . However, BSFC increases considerably with richer than stoichiometric conditions, as expected. Leaner mixtures, for example, $\Psi:0.65$ decreases BSFC and NO_x simultaneously for both SI and LI. Additionally, LI system dropped NO_x from a peak of 44 g/kW h to 5 g/kW h (89% drop) for similar BSFC levels (205 g/kW h). This was a significant benefit considering SI could only drop NO_x from 39.5 g/kW h to 12 g/kW h (70% drop). Therefore, optimizing LI to realize these benefits is deemed necessary. LI coupled with ASM technology holds significant promise once developed for production engines.

7 Combustion Characteristics

High-speed in-cylinder pressure data were acquired to analyze the combustion process for ASM supplied NEA with SI and LI. Cylinder pressure was averaged over 100 consecutive engine cycles for this purpose. A "REV-R" commercial combustion analysis program was used to calculate the parameters such as ignition delay, combustion duration (5–50% MFB), peak cylinder pressure, and COV_{IMEP} .

Figure 13 shows the ignition delay, represented in crank angle degrees (CADs), as a function of Ψ . Ignition delay is defined as the time between the start of ignition (IT) and the start of combustion. The start of combustion was chosen to be 5% MFB. Mass fraction burn is defined as the instantaneous burned mass normalized by the total mass of charge in the cylinder. As shown in the figure, ignition delay increases from 14 deg to as high as 30 deg as Ψ approaches the lean limit. Natural gas inherently has a long ignition delay compared with other fuels. As a result of NEA slowing the chemical reaction rates, it was observed that ignition delays were prolonged even further with 2% NEA compared with standard air.

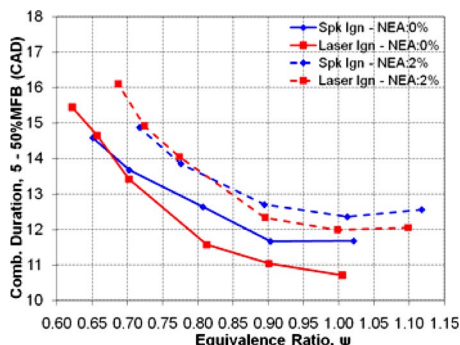


Fig. 14 Combustion duration as a function of ψ

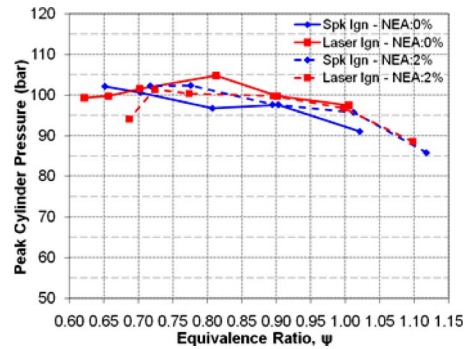


Fig. 15 Peak cylinder pressure as a function of ψ

Combustion duration, the time between 5% and 50% MFB, gives insight into the nature of heat release rates for a given fuel/ O_2 mixture. Figure 14 shows combustion duration as a function of Ψ . As expected, the combustion duration increases exponentially with leaner mixtures. Leaner mixtures result in slower burn or heat release rates for extended periods of time. The lower burning rates are attributed to the slower flame development and propagation speeds caused by NEA. The lower heat release rates and longer combustion duration reduce peak temperatures and hence NO_x emissions.

Figure 15 shows trends for peak cylinder pressures at different Ψ . Both extreme conditions result in pressure drop due to misfires at the lean end and incomplete combustion beyond stoichiometric condition.

COV_{IMEP} , a parameter used in the industry to measure engine stability was maintained below the accepted value of 5%, as shown in Fig. 16. However, even though LI extends the lean limit to 0.62, COV_{IMEP} just begins to increase relative to other conditions.

Figures 17 and 18 are very similar in that both display the

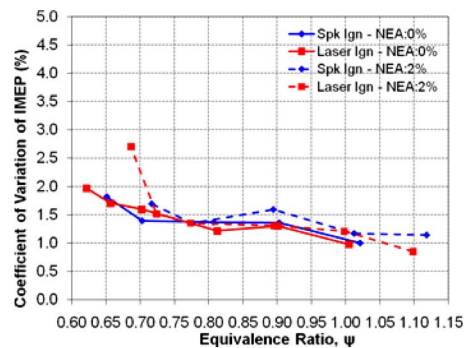


Fig. 16 COV_{IMEP} as a function of ψ

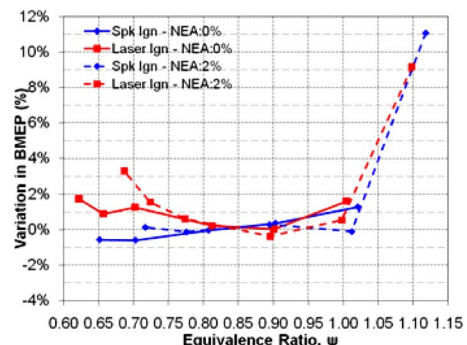


Fig. 17 Variation in load, BMEP, as a function of ψ

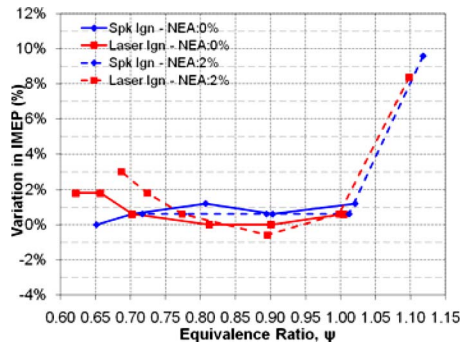


Fig. 18 Variation in load, IMEP, as a function of ψ

variation in BMEP and IMEP from a constant value. However, BMEP was calculated based on actual brake torque measurement, while IMEP was calculated from in-cylinder pressure measurement. The trends in both figures match well, confirming the analysis discussed above. A significant drop in power was observed when Ψ exceeded 1.0. It is highly unlikely for engines to operate at this condition for any period of time. Toward the lean end, it was observed that occasional misfires have to be checked by either shifting slightly richer or advancing ignition timing even further.

8 Conclusions

A single-cylinder spark-ignited natural gas engine was used to study the effect of NEA, ignition timing, and the operating regime of the engine, namely, ψ for SI and LI. The results obtained lead to the following conclusions.

1. N_2 enrichment using ASM could be an effective alternative to EGR.
2. N_2 enrichment lowers NO_x primarily due to LTC.
3. NO_x reductions were between 20% and 89% based on operating regime.
4. Currently operational stoichiometric engines in conjunction with ASM could reduce NO_x emissions by an order of magnitude with minimal hardware modifications (after optimizing the operating region).
5. NEA extends the benefits of lean combustion even further.
6. CO_2 emissions decreased noticeably with 2% NEA. Significant benefits can be realized by lean operation along with NEA.
7. Laser ignition along with N_2 enrichment extended the lean operational limit from ψ :0.72 to 0.68. With standard air, LI extended the lean limit from ψ :0.65 to 0.62.
8. A pressure drop close to 9 kPa was observed on account of ASM installation. This is expected to drop BTE from current presented levels.
9. Usage of ASM to supply NEA to engines is proven to reduce NO_x at all operating conditions.
10. LI system improvement shall be explored further to compensate for loss in BTE at lean conditions, which will be presented at a later time.

Acknowledgment

Argonne National Laboratory's work was supported by the U.S. Department of Energy, Office of Science, Office of Basic Energy Sciences under Contract No. DE-AC02-06CH11357.

Nomenclature

ASM = air separation membrane
 BMEP = brake mean effective pressure
 BSFC = brake specific fuel consumption

BTDC = before top dead center
 BTE = brake thermal efficiency
 CAD = crank angle degrees
 CDI = capacitance discharge ignition
 COV_{IMEP} = coefficient of variation of indicated mean effective pressure
 HCCI = homogeneous charge compression ignition
 IMEP = indicated mean effective pressure
 IT = ignition timing
 LI = laser ignition
 LTC = low temperature combustion
 MBT = maximum brake torque
 MFB = mass fraction burn
 NEA = nitrogen enriched air
 OEA = oxygen enriched air
 PID = proportional integral differential
 PM = particulate matter
 PWM = pulse width modulation
 SI = spark ignition
 TDC = top dead center
 UHC = unburned hydrocarbon
 Ψ = oxygen based equivalence ratio
 Φ = equivalence ratio

References

- [1] <http://www.epa.gov/air/emissions/nox.htm>
- [2] Stanglmaier, R. H., and Roberts, C. E., 1999, "Homogeneous Charge Compression Ignition (HCCI): Benefits, Compromises, and Future Engine Applications," SAE Paper No. 1999-01-3682.
- [3] Karim, G. A., 1983, "The Dual Fuel Engine of the Compression Ignition Type—Prospects, Problems and Solutions—A Review," SAE Paper No. 831073.
- [4] Krishnan, S. R., Biruduganti, M., Mo, Y., Bell, S. R., and Midkiff, K. C., 2002, "Performance and Heat Release Analysis of a Pilot-Ignited Natural Gas Engine," *Int. J. Engine Res.*, **3**(3), pp. 171–184.
- [5] Biruduganti, M., 2002, "Effect of Injection Timing and Pilot Quantity on the Performance of a Dual Fuel Engine," MS thesis, University of Alabama, Tuscaloosa, AL.
- [6] Krishnan, S. R., Srinivasan, K. K., Singh, S., Bell, S. R., Midkiff, K. C., Gong, W., and Will, M., 2004, "Strategies for Reduced NO_x Emissions in Pilot-Ignited Natural Gas Engines," *ASME J. Eng. Gas Turbines Power*, **126**, pp. 665–671.
- [7] Winston Ho, W. S., and Sirkar, K. K., 1992, *Membrane Handbook*, Chapman and Hall, New York.
- [8] Poola, R. B., Stork, K. C., Sekar, R. R., Callaghan, K., and Nemser, S., 1998, "Variable Air Composition With Air Separation Membrane: A New Low Emissions Tool for Combustion Engines," *SAE Trans.*, **106**, pp. 332–346.
- [9] Poola, R., and Sekar, R., 2001, "Simultaneous Reduction of and Particulate Emissions by Using Oxygen-Enriched Combustion Air," *ASME ICE*, Vol. 37-1.
- [10] Kopecek, H., Wintner, E., Pischinger, R., Herdin, G. R., and Klausner, J., 2000, "Basics for a Future Laser Ignition System for Gas Engines," 2000 ICE Fall Technical Conference, ICE Vol. 35-2, pp. 1–9.
- [11] Bosch, R., 1999, *Gasoline Engine Management*, 1st ed., Robert Bosch GmbH, Germany.
- [12] Hiltner, J., Agama, R., Mauss, F., Johansson, B., and Christensen, M., 2000, "HCCI Operation With Natural Gas: Fuel Composition Implications," *ASME Paper No. 2000-ICE-317*.
- [13] Wong, H. C., Beck, N. J., and Chen, S. K., 2000, "The Evolution of Compression Ignition Natural Gas Engines for Low Emission Vehicles," *ASME Paper No. 2000-ICE-318*.
- [14] U. S. Patent No. 5,587,630 and 5,568,801.
- [15] Matthews, R. D., Hall, M. J., Faidley, R. W., Chiu, J. P., Zhao, X. W., Annezer, I., Koenig, M. H., Harber, J. F., Darden, M. H., Weldon, W. F., and Nichols, S. P., 1992, "Further Analysis of Railplugs as a New Type of Igniter," Society of Automotive Engineers International Fuels and Lubricants Meeting, SAE Paper No. 922167.
- [16] Gupta, S. B., Klett, G., Biruduganti, M., Sekar, R. R., Saretto, S. R., Pal, S., and Santoro, R. J., 2004, "Laser Ignition for Natural Gas Reciprocating Engines: A Literature Review," *CIMAC 2004*, Paper No. 204.
- [17] Biruduganti, M., Gupta, S., and Sekar, R., "Low Temperature Combustion Using Nitrogen Enrichment to Mitigate NO_x From Large Bore Natural Gas-Fueled Engines," *ASME Paper No. ICES2008-1616*.
- [18] Phuoc, T. X., 2000, "Laser Spark Ignition: Experimental Determination of Laser-Induced Breakdown Thresholds of Combustion Gases," *Opt. Commun.*, **175**, pp. 419–423.
- [19] Biruduganti, M., Gupta, S., McConnell, S., and Sekar, R., 2004, "Nitrogen Enriched Combustion of a Natural Gas Engine to Reduce NO_x Emissions," *ASME Paper No. ICEF2004-843*.